SAND2021-3699C

Design Considerations for Commercial Scale Particle-Based Thermal Energy Storage Systems

Jeremy N. Sment[1, a)], Timothy Harvey[2, 3, b)], Kevin J. Albrecht[1,c)], Clifford K. Ho[1,d)], Murphy Davidson[4,e)], Kevin J. Albrecht[1], Clifford K. Ho[1], Matthew Lambert[4,f)], Bradley Bateman[5,g)]

[1]Sandia National Laboratories, 1515 Eubank Blvd. NE, Albuquerque, NM, 87123-1127 USA
[2]SSI Consulting, Columbus, OH, USA
[3]Matrix PDM, 445 Hutchinson Ave., Ste. 740, Columbus, OH 43235-5656 USA
[4]Allied Mineral Products, 2700 Scioto Parkway, Columbus, OH 43221 USA
[5]Dome Technology, 4946 N. 29th E, Idaho Falls, ID 83401 USA

[a)]Corresponding author: jsment@sandia.gov
[b)]tharvey@ssiconsultingllc.com
[cd)]kalbrec@sandia.gov
[ed)]ckho@sandia.gov
[ec)]mdavidson01@alliedmin.com
[f)]matthew.lambert@alliedmin.com
[g)] bradley.bateman@dometechnology.com

[d)]kalbrec@sandia.gov
[e)]ckho@sandia.gov

Abstract. Particle-based heat transfer materials used in concentrating solar power systems benefit from gravity-fed arrangements such as vertically integrated components inside the receiver tower which can eliminate the need for conveyance machinery. However, the amount of particles required for commercial scale systems near 100 MW_e can require towers with very thick walls that must be built with high-strength concrete. Cost models for particle-based receiver towers with internal particle storage are being developed in this work and compared to well-established cost models that have been used to estimate tower costs for molten salt systems with external storage tanks. New cost models were developed to accommodate the high-temperature applications required for CSP. Further research is needed to directly compare costs between tower-integrated and external storage. For now, a method is proposed to superimpose increased storage costs with existing molten salt CSP towers. For instances where suitable materials are unavailable or do not meet the structural requirements, ground based storage bins must be used in concert with mechanical conveyance systems. Ground based storage vessels have been shown to be consistent with low thermal energy storage cost and heat loss goals. Ground based storage vessels are well-established in industry.

INTRODUCTION

The peak efficiencies of concentrated solar power (CSP) plants are partly limited by the maximum temperatures that can be handled by either the heat transfer medium such as salts, which begin to break down above ~600° C, and the receiver pipes which may become damaged if temperatures exceed material limits. Solid particle receivers provide an opportunity to bypass piping and directly irradiate a curtain of falling ceramic particles. This enables plants to run concentrating solar tower receivers at higher temperatures (~800° C) resulting in increased CSP system efficiencies.

Sandia National Laboratories is a multimission laboratory managed and operated by National Technology & Engineering Solutions of Sandia, LLC, a wholly owned subsidiary of Honeywell International Inc., for the U.S. Department of Energy's National Nuclear Security Administration under contract DE-NA0003525.

Particle-based heat transfer media also has beneficial characteristics related to thermal storage as the high specific heat and low conductivity create self-insulating behavior and reduce insulation costs. Particle-based storage containers have weights and volumes similar to molten salts, but the inability to pump particles incentivizes the use of gravity-based vertical integration into the receiver tower as is being proposed by the National Solar Thermal Test Facility (NSTTF) at Sandia National Laboratories in Albuquerque, NM, as part of the Generation 3 Particle Pilot Plant (G3P3) project [1]. Previous work has shown the benefits of a flat bottom storage bin design that induces funnel flow in the particle bed to protect the walls from erosion, reduces costs and heat loss associated with a conventional elongated mass flow hopper, and uses stagnant particles on the floor around the outlet as a protective and insulative layer [2]. This study looks at commercial-scale designs and explores the limits of storage capacity that can be practically stored in a tower as well as ground-based storage solutions such as monolithic concrete domes.

The storage capacity is selected to meet system configurations described in the Gen 3 Pathway and prior technoeconomic analyses by Albrecht et al who propose that levelized cost of electricity (LCOE) approaching \$0.06/kWh$_e$ may be achievable with a 100 MWe system with a particle-to-sCO2 heat exchanger and ground-based hot and cold bins with 14 hours of thermal energy storage (TES) [3, 4]. The assumed temperature delta across the heat exchanger is based on the most current G3P3 system design at 160° C. The particles are assumed to be CARBO HSP 40/70 which have a bulk specific heat of 1243 J*g^{-1}*K^{-1}. The bins are modeled to be external and assume a function for conveyance from the storage bin to the heat exchanger and from the heat exchanger to the cold storage bin. Albrecht acknowledges that there is an unknown breakpoint where the cost of supporting large volumes of particles in the tower exceeds the cost reductions gained by eliminating conveyance machinery between the ground-based components. Albrecht also identifies the need for future studies to evaluate the trade-off in construction cost and heat loss when changing the height to diameter ratio of storage bins and thus the effective surface area of the particle formation. This work does not definitively close those gaps but does present first steps toward the development of a tool that can be used to understand the magnitude of the commercial storage material costs in both tower-integrated and external storage designs. Conveyance costs are not discussed herein.

Tower costs used in the Albrecht model are estimated from the work of Buck [5] who gives a cost function for towers as $C_t = 128H_t^{1.9174}$ and a function for an area-specific and temperature-specific insulated structure cost as $C_{stc} = A_{stc}C_{A,sp,is}(T_{r,ex}) + A_{stc}C_{A,sp,is}(T_{r,in})$. The System Advisor Model (SAM) also provides information on material costs for CSP towers [6]. Actual costs for tower construction are highly dependent on location specific factors such as labor, ground conditions, seismicity, and access to raw materials such as concrete. The International Building Code and American Concrete Institute provide codes and specifications for tower construction and include design factors to accommodate the site specific conditions [7], [8]. This study attempts to illustrate how cost models for receiver towers may need to shift when CSP components are integrated due to the inclusion of refractory insulation, higher strength concrete, and additional wall thicknesses and reinforcing steel required to support the components and heat transfer material.

TOWER-INTEGRATED SYSTEM

Tower-integrated systems provide a simple means of routing particles through the system via gravity thus eliminating the cost and maintenance of particle handling and conveyance machines, land use, and structural housing of the CSP equipment. This study investigates cost and structural requirements needed to support a receiver tower with integrated solar components.

Tower Dimensions

Conceptual tower designs have been developed with both the hot and the cold storage bins enclosed within the tower. This study chose a range of cylindrical tower heights from 75-300 m. The inner tower diameters ranged from 10 m to 50 m at the storage bin walls. The concrete walls of each slipform segment varied in 15 cm (6 inch) increments and were designed to be the minimum thickness sustainable for a given height, loading and regional seismicity up to 182 cm (6 feet) which is believed to be the maximum practical thickness for slipform tower construction. The CSP components were arranged as shown in FIGURE 1 with the cold storage at ground level and turbomachinery, heat exchanger and hot storage bin vertically integrated above. The hot bin was suspended by up to a~~n~~ 1.4 m (6 ft) thick slab an inverted cone and for additional floor support [9]. Size and weight of the CSP components were considered in determining the heights and thicknesses of the floors. No considerations were made for component or system integration in this study. The concept used in the external storage discussion is shown on right.

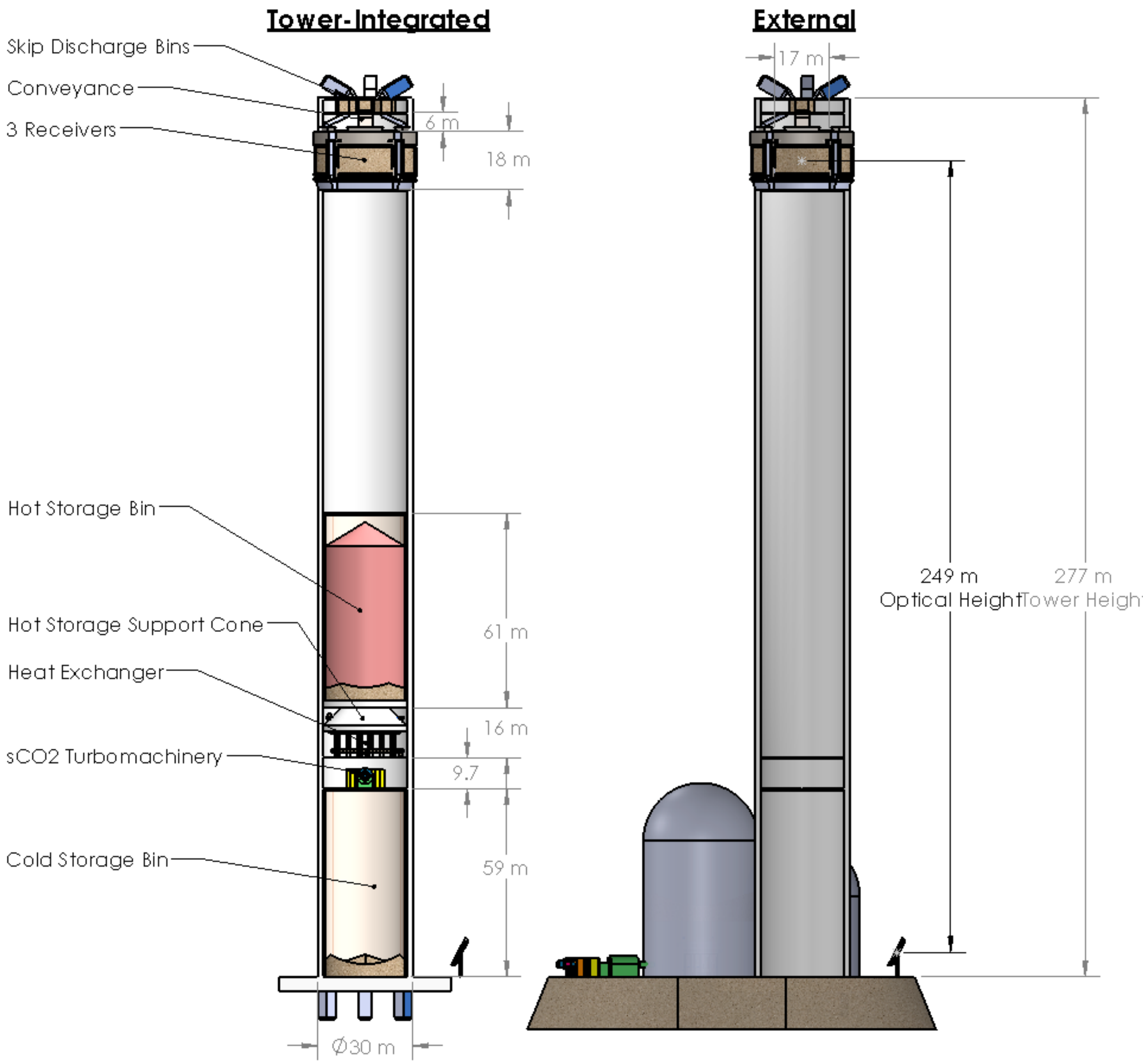

FIGURE 1. Tower-integrated CSP component dimensions for 25 m diameter 250 m height

CSP Component Sizing and Loads

Storage capacity was variable and determined as a function of tower height. Albrecht et. al. have shown that 14 hours of storage for baseload plants are one of many possibilities that are consistent with a desirable LCOE [3]. This study selected 14 hours as the deferred storage duration. The thermal capacities as a function of tower height were derived from the relationship shown in FIGURE 2 which is derived from optical height requirements found in relevant falling particle receiver literature for 10 MW_e [10], 50 MW_e [11], and 100 MW_e [1] receiver systems. Table 1 summarizes the values derived.

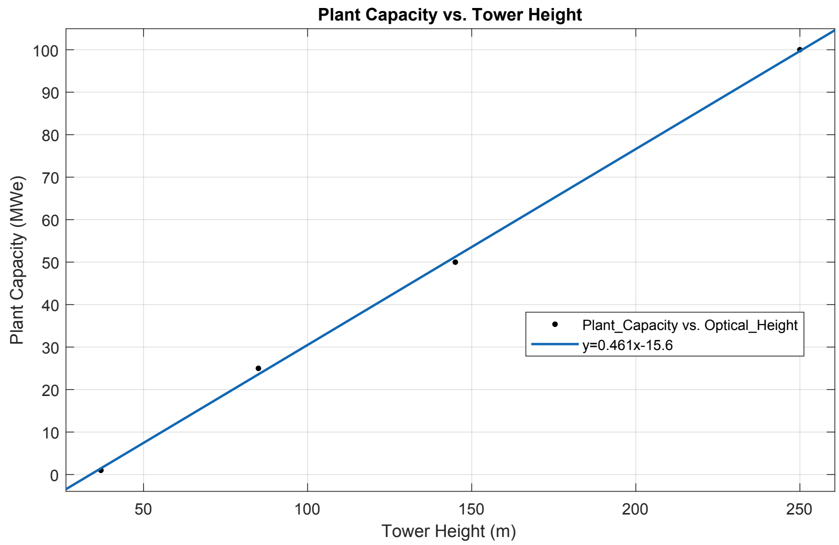

FIGURE 2. Assumed thermal capacity as a function of tower height

Table 1. Tower Height and Capacity

Source	Plant Capacity (MW_t)	Solar Multiple	Receiver Design Point (MWt)	Optical Height (m)
G3P3 [1]	1	2.5	2.5	37
10 MWe [10]	22	1.3	31.2	85
50 MWe [11]	122	1.2	150	145
100 MWe [1]	200	2.75	550	250

The components were sized as follows:

- Receiver: Systems >150 m or >50 MWe were loaded with three receivers at 100,000 kg each. Each receiver sub-system included a feed-hopper weighing a combined 133,000 kg and three skips on top of the roof with 84,000 kg of particles each. A mechanical conveyance system and particle chutes were considered weighing a combined 276000 kg. For capacities <50 MWe (≤100 m towers), a single 1/10 scale ~~1~~ receiver sub-system was modeled. ~~For the 75 m tower, a single 1/10th scale receiver sub-system was modeled.~~
- Hot Storage: The method to determine storage capacity is described above. The 100 MW_e system had an active heat transfer material volume of 23,500 m^3 ~~and weighed~~weighing 50.7 million kg [12]. The volume and weight~~height~~ of the storage bin materials varies as a function of bin diameter and capacity. The following assumptions were used to size the storage bin:
    - Thermal to electric conversion of sCO_2 turbine = 0.5
    - ΔT of particles across heat exchanger = 160° C
    - Packed bulk density = 1235 kg/m^3
    - Average c_p from 615° to 775° C = 1243 J/g/K
    - Angle of repose = 31.3° C
    - Drawdown angle = 30° C
- Heat Exchanger: A bank of 16MW_t heat exchangers weighing ~34,000 kg each designed by *Solex* and *VPE* was located beneath the hot storage support. The weight was scaled to capacity in units of 16 MW_t. An additional 25% weight was assumed for the conveyance system above the heat exchanger. The height was 13.8 m.

- Power block: The sCO_2 heat exchanger and turbomachinery was modeled on equipment weight estimates for power loops from 25-300 MW_e by Gibbs et. al. (FIGURE 3) [13]. The height was estimated to be 6.5 m for all instances.
- Cold Storage: The cold storage bin was assumed empty except for the stagnant drawdown region which is described in detail below.

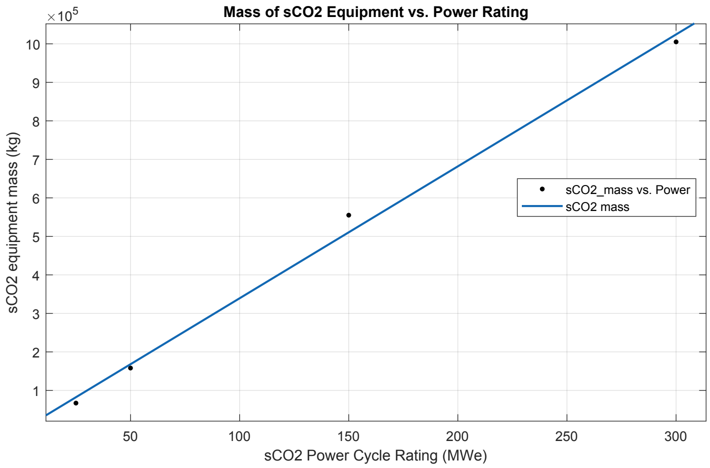

FIGURE 3. Estimated mass of sCO_2 loop including heat exchangers, turbomachinery, pipes and valves as a function of power rating

Storage Bin Walls and Insulation

The storage bin design included a 0.1 m layer of high-density (2210 kg/m^3) refractory for strength and erosion resistance followed by a 0.5 m thick layer of low-density (640 kg/m^3) refractory with increased thermal resistance. Both refractories are assumed to cost 2700 \$/m^3. A thin 0.05 m layer of microporous insulation (270 kg/m^3) at \$17000/m^3 is considered to maintain surface temperatures at the structural tower walls below 100° C and to accommodate thermal expansion from the bin. Microporous insulation has no effective modulus of elasticity and must be sized such that it cannot be compressed more than 10% of its initial dimensions. **Error! Reference source not found.** FIGURE 4 shows a cutaway view of the bin and the relative cost contributions from the storage bin walls, floor, and ceiling. The change in cost slopes are a result of tower diameter increase as required. The ceiling of the bins is insulated with a 0.3 m layer of ~~silica~~ aluminosilicate fiber modules with a density of 220 kg/m^3. The cost of the support cone, and 2.4 m thick floor are included below as additional tower costs.

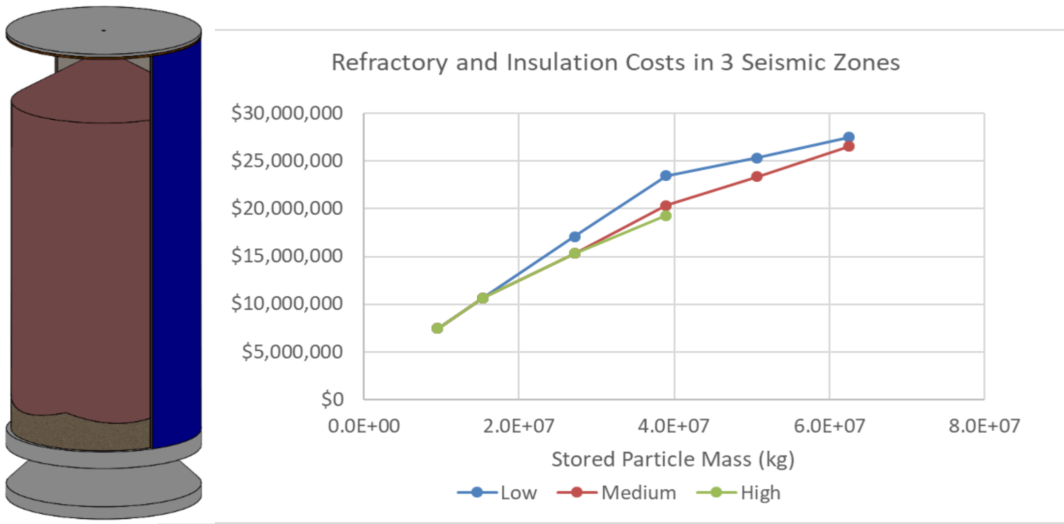

FIGURE 4. (Left) Storage bin cut-away view with insulation, flooring material and support cone. (Right) Storage refractory and insulation costs in low, medium and highly seismic regions

Storage Bin Flooring Material

Methods to reduce the cost and weight of the flooring material were evaluated. Flat-bottomed storage bins may be less costly than self-evacuating hoppers with sloped floors. However, the quantity of particles remaining on the floor around the outlet can be substantial. The volume and mass of the drawdown region as a result of multiple outlets was determined using CAD as shown in FIGURE 5.

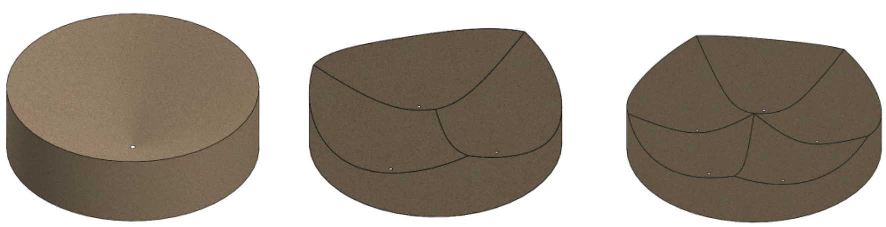

FIGURE 5. Formation of stagnant particles remaining on bin floor after discharge with 1, 3, and 5 outlets

The volume of stagnant materials could be replaced with a lighter and lower cost material. As an example, lava rock gravel (bulk density = 1430 kg/m^3) that is commonly available for landscaping was assumed to occupy 90% of the volume of the stagnant region. Particles (bulk density = 2135 kg/m^3) would then be poured over to facilitate the desirable flowability and low erosion properties from particle on particle flow. Particles are assumed to occupy the upper 10% of the volume. FIGURE 6 shows the relative cost of flooring material if particles are assumed to be CARBO HSP 40/70 at ~~1~~ 2135 $/~~kg~~ m^3 and lava rock is assumed to be ~~0.30~~429 $/~~kg~~m^3. Mass and costs of flooring with and without filler material are shown in red and the trend of volume reductions from increasing the number of outlets is shown from left to right. The blue bars represent the cost with the assumed filler material.

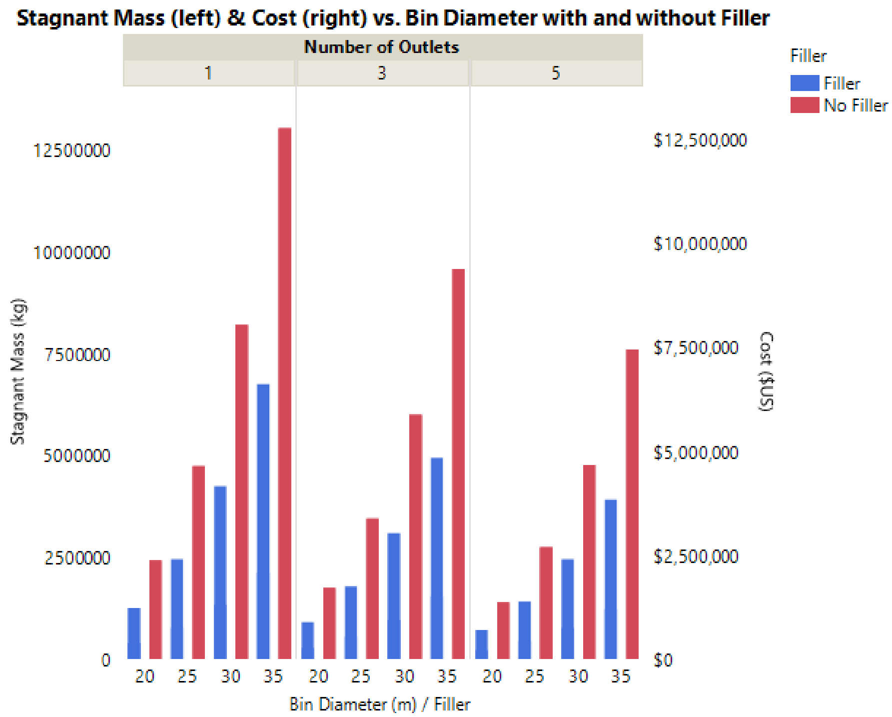

FIGURE 6. (Above) Modeled drawdown regions with 1, 3, and 5 outlets. (Below) Overlay of mass of drawdown region as a function of bin diameter for 1, 3, and 5 outlets with all particles and with a lightweight filler

Tower Structure Model

A tower model was developed to evaluate the feasibility of tower construction with integrated CSP components [9]. The tower is made of reinforced concrete. The conceptual design of the tower has been performed using the requirements of the International Building Code (IBC) [7], the American Concrete Institute (ACI) 318-14 Building Code Requirements for Structural Concrete and the ACI 313-16 Design Specifications for Concrete Silos and Stacking Tubes for Storing Granular Materials [8].

The extreme height and mass of the tower results in a structure that is sensitive to seismic action. The lateral shear and overturning moment of the tower structures have been estimated per the requirements of the IBC, given the proposed locale of the structure. The fundamental period of vibration of the tower used in the overturning analysis has been estimated using a numerical integration technique developed by C.E. Freese for vertical pressure vessels [14].

The thickness of the tower shell and the vertical reinforcement in the wall are a maximum at the base of the tower and may be reduced as the height of the tower increases. The circumferential reinforcement in the shell wall is a maximum in the bin storage regions, where the shell is designed per the ACI 313-16 requirements.

The lower storage bin is located at grade and may be supported directly on the tower foundation or on columns from a lower structural level. In towers with both the hot and cold materials enclosed in the tower, the presence of the lower bin precludes the use of supporting interior columns that would penetrate the lower storage bin. The bottom floor of the upper storage bin must be entirely supported by the exterior tower cylindrical shell. In towers with diameters > 25 m, an inverted conical support structure is proposed to provide interior support for the bin floor.

The large tower loads and potentially large seismic overturning moments result in significant foundation loads. Site specific geotechnical investigations will be required to determine the optimal foundation support system for the proposed towers. Should large at-grade soil bearing pressures not be achievable, deep foundations utilizing piles or caissons are anticipated. In this study foundations were assumed to have a diameter equal to the greater of 20% of the tower height or 4/3 of the tower diameter with a thickness of 1/60th the height of the tower.

Tower Cost Analysis

Material costs for integrated towers will be higher than current cost models based on molten salt towers with external storage due to the following:

- Increased wall, floor, and foundation thickness and required steel reinforcement – primarily to support the additional weight of storage. Other component loads were shown to have a relatively minor effect.
- Increased tower diameters needed to maintain a suitable height to diameter ratio of the storage bin that can fit under the required receiver height.
- Increased height required to accommodate skip discharge bins and sloped particle ducts from the skips at the rear of the tower to the receiver

While a comprehensive particle-based tower design is the subject of future work, the structural model has been adapted to provide parametric estimates of these cost increases from the required volume of concrete and steel. It is assumed that the increase in costs is only a matter of structural tower materials and that all other constituents of tower costs such as labor, crane mobilization, slipform mobilization etc. would remain constant. With this assumption, the total tower costs can be derived by superimposing the tower cost increase with existing comprehensive cost models that have been developed for molten salt systems with external storage such as a 2017 study by Schlaich Bergermann & Partner (SBP) [5, 15], and the cost function provided by the System Advisor Model (SAM) [6]. Specific material costs will vary as a result of market rates and access to water. A value of 230 $\$/\text{m}^3$ for concrete and 1000 $/tonne for reinforcing steel was adopted for this study. A cost correlation for high-strength concrete is given by the US Department of Transportation [16]. High-strength concrete >45 MPa (6,000 psi) may not be suitable for slipform concrete construction as it must be pumped to great heights and is more likely to fast-set. With the use of retardants, strengths up to 48.3 MPa (7000 psi) might be possible.

This strength is assumed to be the maximum limit in this study. Furthermore, concrete may be difficult to obtain, and shipping and delivery costs may make their use prohibitive. A batch plant can be installed for approximately $2M if a significant source of water is available. The study assumes that the maximum wall thickness for a slipform construction method is 1.8 m (6 ft). When a solution could not be found where the required strength < concrete strength at the thickness limit, the diameter was increased which had the effect of lowering the center of mass and thus the overturning moment.

To estimate the cost associated with the increased materials, the model was run with and without integrated components in a range from 75 m to 300 m. FIGURE 7 shows the combined cost of concrete walls, foundation, and reinforcing steel. As a point of comparison, tower cost relationships for a system with external storage from Buck and Albrecht are shown with square markers [5].

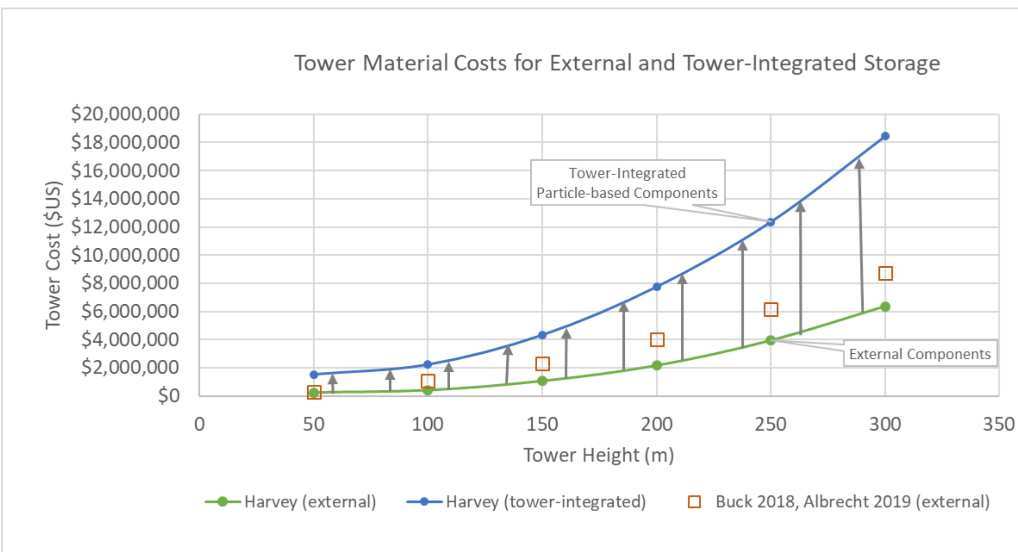

FIGURE 7. Tower material costs vs. height for towers with and without integrated components. ~~Material c~~Costs provided by Buck et. al.~~from a molten salt based study by SBP~~ are shown in red squares.

Seismicity Considerations

Solutions for towers with no integrated storage were found for towers as low as 10 m in diameter. Integrated systems required increased diameters to keep the stored mass in the hot storage bin as low in height as possible. Designs where the top of the hot storage bin is less than 2/3 of the tower height are most successful. FIGURE 8 shows the particle tower model costs in representative locations with low, medium and high seismicity. In Daggett, CA, the most seismic region considered, a solution could not be found for the variable mass scenario above ~178 m. Here, the maximum feasible capacity for a tower-integrated system with two storage bins is a 35 MW_e with 6 hours of thermal energy storage (420 MWh_t) [17]. The dashed curves show the results of towers with no storage and solid lines represent the tower-integrated configuration.

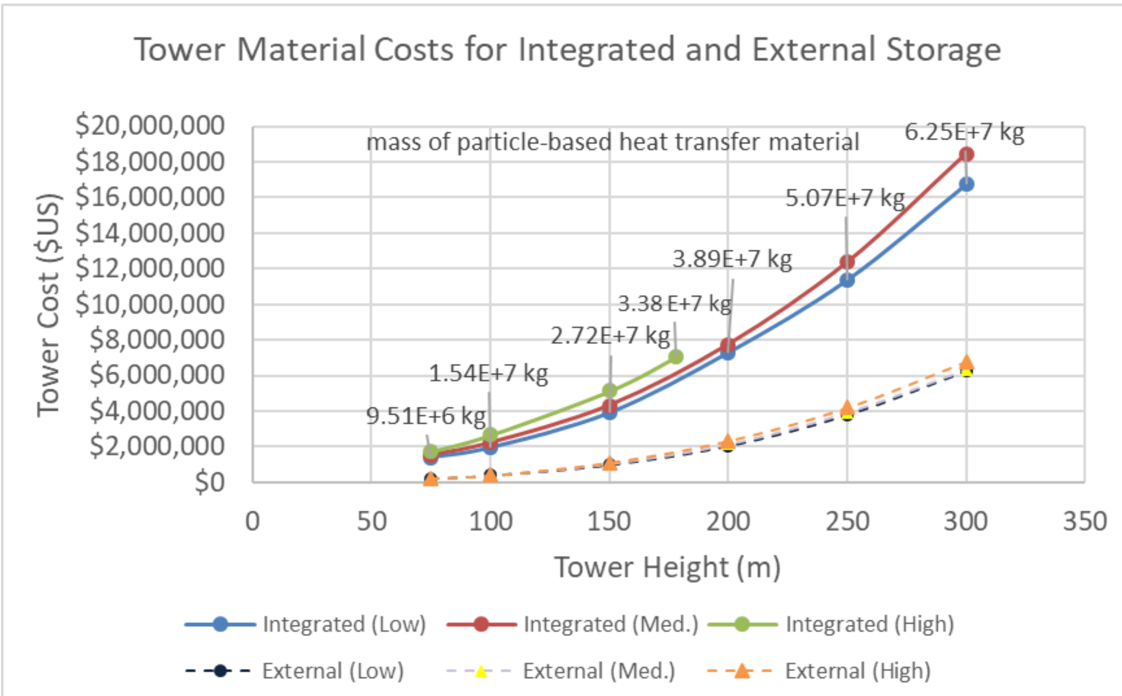

FIGURE 8. Costs of towers in regions with low, medium, and high seismicity with external and tower integrated storage. The mass of the particles is height-dependent and indicated with data labels.

Given the sensitivity to a region's seismicity, the viability of integrated towers was assessed by running the model with seismic conditions, and storage capacities similar to eight CSP tower systems around the world as shown in TABLE 2 and FIGURE 9 [18]. The majority were located in China in areas with low seismicity [19]. Noor III is in an area of Morocco with low seismicity [20]. Crescent Dunes had a high seismicity but slightly less than Daggett, CA [21]. The algorithm for particle-based tower heights shown in FIGURE 2 was used to adjust the molten salt receiver tower heights to particle receiver heights and the mass of the components were calculated based on the storage capacity. In all situations, a particle-based tower geometry would have been viable.

TABLE 2. Representative commercial CSP plants with molten salt storage

Site Name	Location	Net Capacity (MW_e)	Tower Height (m)	Storage Capacity (hr)
Crescent Dunes	Tonopah (US)	110	195	10
Hami	Hami (CN)	50	180	8
Luneng Haixi	Haixi Zhou (CN)	50	188	12
NOOR III	Ouarzazate (MA)	134	250	7.5
Qinghai Gonghe	Gonghe (CN)	50	171	6

Shouhang Dunhuang Phase I	Jiuquan Shi (CN)	10	138	15
Shouhang Dunhuang Phase II	Jiuquan Shi (CN)	100	220	11
SUPCON Delingha	Haixi Zhou (CN)	50	200	7

FIGURE 9. Locations of Solar Towers. Comparable molten salt towers with TES used in TABLE 2 have been indicated with blue circles. [18]

Cost Factors for Tower-Integrated Storage

To derive a cost estimate for a particle-based integrated tower, a curve was fit to the differences between external and tower-integrated storage costs as shown in FIGURE 7 and superimposed with a comprehensive molten-salt tower cost-height relationship. The structural cost factors for this study are shown in FIGURE 10 and are specific to the loading and locations of a specific tower and should not be generalized without these considerations.

For the specific system design proposed, the cost relationship is taken from the study led by SBP [15]. The SBP study was based on a structure in a region with medium seismicity and is superimposed with the "medium" material cost increase curve as:

$$C_{SBP,particle} = 235 * H_{tower}^{1.87} + 3.16E5$$

A higher cost relation is created using the SAM tower cost model, subtracting the cost of piping (given in the SBP report), and adding the material cost increase. $C_{SAM,particle} = 304 * H_{tower}^{1.87} + 5.79E5$

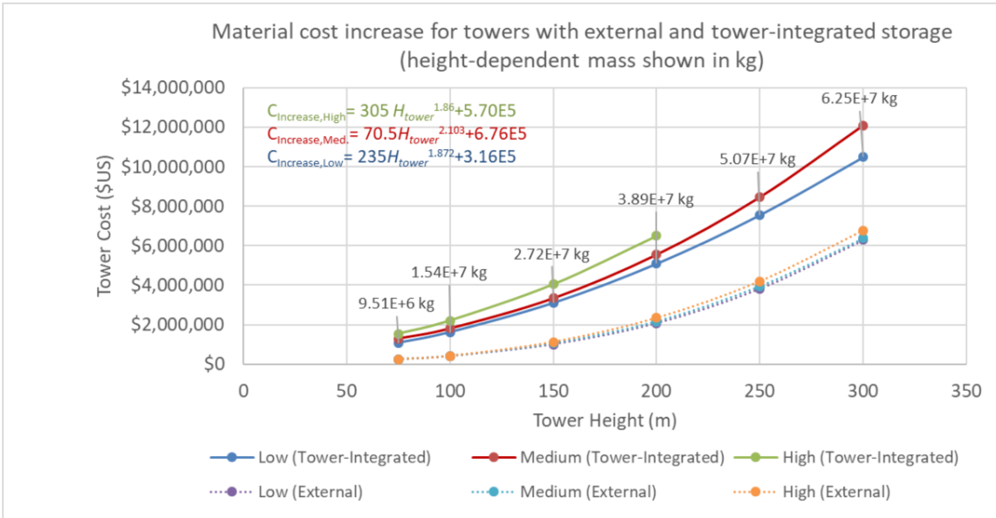

FIGURE 10. Cost increase of towers with integrated storage relative to a tower of equivalent height with external storage bins. Mass of heat transfer material is shown in data labels and is constant for all seismicities.

~~For the specific system design proposed, the cost relationship is taken from the study led by SBP [15]. The SBP study was based on a structure in a region with medium seismicity and is superimposed with the "medium" material cost increase curve as:~~

$$C_{SBP,particle} = 235 * H_{tower}^{1.87} + 3.16E5$$

~~A higher cost relation is created using the SAM tower cost model, subtracting the cost of piping (given in the SBP report), and adding the material cost increase.~~ $C_{SAM,particle} = 304 * H_{tower}^{1.87} + 5.79E5$

External Storage

For towers that are too short and narrow to fit all the CSP components, or too narrow and tall to survive in areas of high seismic activity, external storage may be necessary. Monolithic concrete domes were considered as an alternative to tower-integrated storage (FIGURE 11). Hundreds of domes have been used across several industries since the 1970s providing a significant body of evidence for reliability over life-cycles approaching 30 years. These domes have been used in high-temperature applications such as clinker storage which may initially reach over 1000° C. However, the cyclic use of particle-based heat transfer material >800° C may be novel to the industry. Future work will include effective heat transfer of steel reinforced walls and shotcrete anchors, ground effects, and particle interactions with joints in the walls.

FIGURE 11. Monolithic concrete dome storage vessels. (Left) foundation construction of a large concrete dome with discharge tunnel. (Right) Dome with charging chute. Images are property of Dome Technology and are used with permission.

Two models were used to assess thermal performance of the bins. A preliminary 1-D thermal resistance network was used to determine steady-state conditions and allowed a fast process for adjusting the insulating and structural layer thicknesses. The model accounts for both the cylindrical portion and spherical roof of the proposed bins.

Once the refractory insulation layers were determined, the design was run in a cyclic CFD model described in earlier work [2]. FIGURE 12 shows the results where daily heat loss was found to be <1% in the nominal design scenario which includes 600 mm of refractory insulation and 600 mm of ~~cement~~concrete. Concrete dome and foundation temperatures exceed the 100° C maximum temperature requirement so a heat-resistant concrete (HRC) must be used in tandem with the standard concrete. A high-strength heat-resistant concrete made with ~~Calcium~~ calcium ~~Aluminate~~ aluminate was identified that has strengths up to 62 MPa (9,000 psi) at cyclic temperatures up to 1100° C [22]. The costs were estimated to be about 5.2 times the cost of standard Portland cement-based concrete of similar strength.

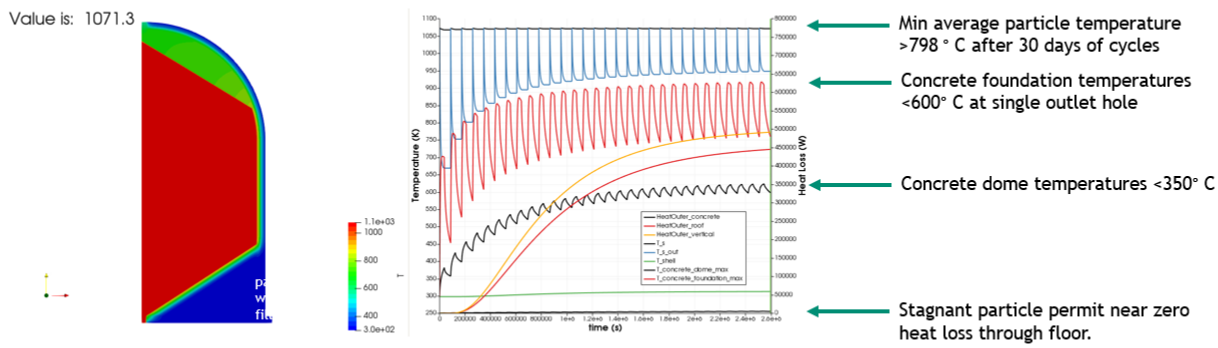

FIGURE 12. Results from cyclic steady state model of concrete monolithic dome.

TABLE 3 shows the basic geometric considerations for the plant capacities used in this study. The 200 and 300 MWt capacities are likely choices for external storage when a single tower is selected. The insulation design was similar to the tower-integrated bins. The flooring material uses a low-cost filler material as described above. The refractory walls had a fixed design with 100 cm of high-density shotcrete applied refractory and 500 cm of low-density shotcrete applied refractory. HRC was used behind the refractory layers and set to a proportion of the required structural wall thickness that kept the ~~cement~~ Portland cement-based concrete below 100° C. TABLE 4 summarizes the costs of the same storage bins. The 200 MW_t (100 MW_e) storage bin with 14 hours of thermal storage has a unit cost of 21 $/$kWh_t$.

TABLE 3. Basic geometry considerations for concrete monolithic dome storage**.**

Plant Capacity (MW_t)	Storage Capacity (hr)	Heat Transfer Material Mass (kg)	Heat Transfer Material Volume (m^3)	Inner Diameter (m)	Ceiling Height (m)	Structural Wall Thickness (m)
20	6	2.2M	1000	12	14	0.25
100	6	11M	5000	20	24	0.4
100	14	25M	12000	27	32	0.5
200	14	51M	24000	34	41	0.6
300	14	76M	36,000	39	47	0.7

TABLE 4. Storage Bin Costs for External TES

Storage Capacity (MWh_t)	Heat Transfer Material (million $US)	2x Nominal Domes (million $US)	2x Bin Insulation Materials (million $US)	Total Cost (million $US)	Area Specific Cost per Bin* ($US/bin/$m^2$)	Stored Energy Unit Cost ($US/$kWh_t$)
120	$1.3 M	$1.40	$2.1	$4.8 M	$3330	$39.7
600	$6.5 M	$3.00	$6.7	$16.2 M	$3030	$27.1
1400	$15.2 M	$5.00	$12.3	$32.5 M	$3170	$23.2

2800	$30.4 M	$7.60	$20.7	$58.7 M	$3140	$21.0
4200	$45.6 M	$9.28	$27.0	$82.8 M	$3180	$19.7

*Cost per area does not include heat transfer media

The majority of the insulation costs were necessary only to protect the surface temperature of the structural concrete. A low-cost scenario was investigated that used HRC for the dome structure eliminating the need to maintain a 100°C surface temperature the structure and freeing the insulation design to serve only the heat loss requirements. As a lower cost bound, particles were considered to be in direct contact with the structural walls. Cyclic CFD modeling ([23]) showed the volumetric average temperature of all particles in an uninsulated bin to be 4.1° C cooler than a similarly shaped bin with 600 mm of insulation and a microporous insulation layer. This is 3 times the relative heat loss of the insulated bin and amounts to 2% of the total required heat. TABLE 5 shows the costs for the same sized bins above with the same flooring concept but without refractory insulation.

TABLE 5. TES costs for 2 bins without insulation

Storage Capacity (MWh_t)	Total Cost (million $US)	Area Specific Cost per Bin* ($US/bin/m^2)	Stored Energy Unit Cost (US/kWh_t$)
120	$3.0 M	$1650	$25.2
600	$11.1 M	$1430	$18.5
1400	$23.8 M	$1510	$17.0
2800	$44.9 M	$1610	$16.1
4200	$65.3 M	$1677	$15.5

CONCLUSIONS AND NEXT STEPS

Material costs for particle-based CSP towers with integrated TES may be higher than some salt-based tower models due to the required wall thickness, higher strength sections of concrete, and insulation. Tower-integrated storage is also limited by tower height and diameter as well as the seismicity of the region.

Particles have the largest impact to overall TES costs followed by the heat exchanger ΔT. Narrow towers (<20 m) can reduce tower materials but may not be an option in areas of high seismicity or for towers with large capacities. It is costly and structurally difficult to add enough refractory insulation to maintain surface temperatures of concrete <100° C. Calcium aluminate-based heat-resistant concrete can survive cyclic temperatures up to 1100° C with compressive strengths > 65 MPa (9000 psi). Thermal models without any insulation show particles lost 3.4% of their heat after 14 hours of storage vs <1% with insulation. TES systems approaching the $15/kWh$_t$ SETO 2030 goal may be feasible if particle inventory could be reduced by increasing achievable ΔTs in the heat exchanger and modest reductions in material costs across the board.

Direct cost comparison of particle-based towers and salt-based towers (SAM, SBP) would be greatly improved by further consultation with tower construction experts who may be able to provide complete cost models which refine existing design assumptions and incorporate labor and other design-specific costs. Cost offsets from the elimination of external storage bins are the subject of other work currently evaluating overall tower-integrated TES system cost models. Integration of heat exchanger and turbomachinery inside the tower has not yet been evaluated other than in terms of volume and weight.

ACKNOWLEDGEMENTS

The authors thank Reiner Buck of DLR for translating the SBP, DLR, and CSP Services documentation and for contributing additional details of the tower designs used to benchmark the particle tower model, Marc Jolin of Laval University, Joe Talley and Chuck Alt from Imerys for contributing to our understanding of heat resistant concrete material properties and costs, and Lane Roberts from Dome Technology for his contributions in designing, pricing, and construction advisement of concrete monolithic domes.

This work is funded in part or whole by the U.S. Department of Energy Solar Energy Technologies Office under Award Number 34211. This report was prepared as an account of work sponsored by an agency of the United States

Government. Neither the United States Government nor any agency thereof, nor any of their employees, makes any warranty, express or implied, or assumes any legal liability or responsibility for the accuracy, completeness, or usefulness of any information, apparatus, product, or process disclosed, or represents that its use would not infringe privately owned rights. Reference herein to any specific commercial product, process, or service by trade name, trademark, manufacturer, or otherwise does not necessarily constitute or imply its endorsement, recommendation, or favoring by the United States Government or any agency thereof. The views and opinions of authors expressed herein do not necessarily state or reflect those of the United States Government or any agency thereof.

Sandia National Laboratories is a multimission laboratory managed and operated by National Technology and Engineering Solutions of Sandia, LLC., a wholly owned subsidiary of Honeywell International, Inc., for the U.S. Department of Energy's National Nuclear Security Administration under contract DE-NA0003525.

REFERENCES

[1. Clifford K. Ho, K.J.A., Lindsey Yue, Brantley Mills, Jeremy Sment, Joshua Christian, Matthew Carlson, *Overview and Design Basis for the Gen 3 Particle Pilot Plant (G3P3)*, in *SolarPACES 2019 Conference Proceedings*. 2019: Daegu, South Korea.

2. Sment, J.N., et al. *TESTING AND SIMULATIONS OF SPATIAL AND TEMPORAL TEMPERATURE VARIATIONS IN A PARTICLE-BASED THERMAL ENERGY STORAGE BIN*. in *ASME 2020 14th International Conference on Energy Sustainability*. 2020. Denver, CO: ASME.

3. Albrecht, K.J., Matthew L. Bauer, and C.K. Ho. *Parametric Analysis of Particle CSP System Performance and Cost to Intrinsic Particle Properties and Operating Conditions*. in *ASME 2019 13th International Conference on Energy and Sustainability*. 2019. Bellevue, WA: ASME.

4. Powers, S., *Gen 3 CSP Topic 1 - Phase 3 Test Facility Down-Selection Criteria*. 2019, United States Departmente of Energy Office of Energy Efficiency and Renewable Energy.

5. Buck, R. and S. Giuliano. *Impact of Solar Tower Design Parameters on sCO2-Based Solar Tower Plants*. in *2nd European Supercritical CO2 Conference*. 2018. Essen, Germany.

6. Turchi, C.S. and G.A. Heath, *Molten Salt Power Tower Cost Model for the System Advisor Model*. 2013: NREL.

7. Council, I.C., *International Building Code (IBC)*, in *IBC2018*. 2018.

8. ACI_Committee_313, *Design Specification for Concrete Silos and Stacking Tubes for Storing Granular Materials*, in *ACI 313-16*, A.C. Institute, Editor. 2016.

9. Harvey, T.A., *100 MW Storage Options Report*. October 13, 2019, Matrix PDM, Engineering.

10. Brantley Mills, C.K.H., *Proposed 10 MWe North-Facing Falling Particle Receiver Design*. 2016, Sandia National Laboratories, U.S. Department of Energy.

11. Brantley Mills, C.K.H. *Annualized Thermal Performance of Intermediate-Scale Falling Particle Receivers*. in *SolarPACES 2017*. 2017. Santiago de Chile.

12. Kevin J. Albrecht, L.Y., Brantley Mills, Jeremy N. Sment, Hendrik F. Laubscher, Joshua M. Christian, Matthew D. Carlson, Clifford K. Ho, *Design Features and System Integration of a Next-Generation Concentrating SOlar Power Particle Pilot Plant*, in *14th International Conference on Energy and Sustainability*. ASME: Denver, CO.

13. J.P. Gibbs, P.H., M.J. Driscoll, *Applicability of Supercritical CO2 Power Conversion Systems to GEN IV Reactors*. 2006, Center for Advanced Nuclear Energy Systems.

14. Freese, C.E., *Vibrations of Vertical Pressure Vessels.* Journal of Engineering for Industry, 1959: p. 77.

15. Weinrebe, G., et al., *Kostensenkung bei Solarturmkraftwerken durch optimeierte Heliostatkonturen plus angepasstes Turm-und Felddesign*. 2019, Schlaich Bergermann Partner (sbp), Deutsches Zentrum Fur Luft- und Raumfahrt (DLR), Concentrating Solar Power (CSP) Services: HELIKONTURplus. p. 110.

16. DOT, U.S., *Optimized Sections for High-Strength Concrete Bridge Girders--Effect of Deck Concrete Strength*. 2006, U.S. Department of Transportation Federal Highway Administration.

17. Harvey, T.A., *Sandia CSP Project Report 13020*. 2020, SSI Consulting, LLC.

18. NREL, *Concentrating Solar Power Projects*, SolarPACES, Editor. 2020.

19. Yu Y., G.m., Xu G. . *Seismic Zonation*. Encyclopedia of Earth Sciences 2011 [cited 2020 October 25, 2020]; Available from: https://link.springer.com/referenceworkentry/10.1007%2F978-90-481-8702-7_184.

20. Taj-Eddine Cherkaoui, A.E.H., *Seismicity and Seismic Hazard in Morocco 1901-2010.* Bulletin de l'Institut Scientifique, 2012. **Sciences de la Terre**(34): p. 45-55.
21. Survey, U.S.G. *Unified Hazard Tool*. Earthquake Hazards Program; Available from: https://earthquake.usgs.gov/hazards/interactive/.
22. *Fondag Product Properties*, K. Inc., Editor., Kernius Inc.
23. Sment, J.N., et al. *Design Considerations for a High-Temperature Particle Storage Bin*. in *SolarPACES*. 2020. Degu, South Korea: SolarPACES.